Published in final edited form as:
Bioorg Med Chem Lett. 2007 September 1; 17(17): 4891–4894.

A Relationship between Amide Hydrogen Bond Strength and Quinone Reduction Potential; Implications for Photosystem 1 and Bacterial Reaction Center Quinone Function

Ken S. Feldman[a], **D. Keith Hester II**[a], and **John H. Golbeck**[a,b]

a*Department of Chemistry, The Pennsylvania State University, University Park, Pennsylvania, USA 16802*

b*Department of Biochemistry and Molecular Biology, The Pennsylvania State University, University Park, Pennsylvania, USA 16802*

Abstract

A series of 11 simple phylloquinone derivatives, each lacking the extended phytyl side chain but featuring H-bond donor amides at one or both peri positions, were prepared and some salient physical properties were measured. A correlation between both IR frequency and NMR peak position, as indicators of internal H-bond strength, and the quinone half-wave reduction potential, was observed. These data are consistent with the prevailing hypothesis that quinone carbonyl H-bonding in general, and stronger H-bonds in particular, favorably bias the endogenous quinone's electrochemical potential toward easier reduction.

The complete structural characterization of the photosynthetic reaction centers Photosystem 1 (PS1)[1] and bacterial reaction center (bRC)[2] has enabled unparalleled advances in understanding the mechanistic underpinnings of photosynthesis.[3] Even as Angstrom-level features have come into focus, the relationship between structure and function, in many cases, has yet to be clarified. One pivotal feature of the light-driven electron transfer from each system's primary chlorophyll acceptor to the terminal repository, a quinone (bRC) or Fe_4S_4 cluster (PS1), involves reaction through an intermediate quinone transfer junction (ubiquinone (**1**) in bRC and phylloquinone (**2**) in PS1), Fig. 1. The critical reduction potentials of these quinones are thought to be responsive to local electrostatic effects, with proximal negatively charged amino acid side chains and a juxtaposed negatively charged iron-sulfur cluster contributing to a lower value (harder to reduce) for phylloquinone in PS1 compared with an adjacent and reduction-facilitating Fe^{2+} site in bRC.[4] In addition to these charge effects, both H-bonding and π-stacking also are cited as influential factors in determining the quinone reduction potential. Ubiquinone is pinioned by the protein matrix between two H-bonds as shown, and so it is not surprising that it's estimated reduction potential in vivo is higher than (more easily reduced than) the same quinone in the non-protic media DMF. Whereas the inexact modeling of a protein interior by DMF does not allow too firm of a conclusion to be drawn, it is likely that at least some of the diminished reduction potential of the in vivo version can be attributed to dual H-bond activation of the quinone's carbonyls. It is quite surprising, then, that the analogous quinone **2** of PS1 exhibits a reduction potential that is substantially *lower* than various phylloquinone models in DMF solution, given that it, too, presumably benefits from the single H-bond shown.[5] The role that the enveloping protein plays in modulating the reduction potential of this quinone has been a matter of speculation, and one theory in current

ascendancy focuses on the protein-mediated modulation of a π-stacking interaction with the adjacent indole ring of TrpA697.[6] From this perspective, the π-stacking interaction is viewed as energetically favorable for the parent quinone, but destabilizing (and yet structurally unavoidable) for the reduced species. Nevertheless, the contributions of the singular H-bond to **2** cannot be ignored, especially when circumstantial evidence suggests that this H-bond, in contrast to the dual H-bonded arrangement exhibited for the analogous quinone **1** in bRC, is particularly strong as a consequence of an extended H-bonding network provided by the protein matrix and associated waters.[7] Thus, the overarching question emerges, how can amide H-bonding, and more precisely, the strength of amide H-bonding, influence a quinone's reduction potential?

The relationship between H-bond strength and quinone reduction potential[11] was probed using simple model 5-amido and 5,8-diamidonaphthoquinones. This approach is precedented by a long history of studying the relationship between the reduction potential of ortho hydroxy- and amino substituents on benzo- and naphthoquinones,[12] and peri-positioned hydroxy, and in a few examples amino,[13a] groups on naphtho- and 9,10-anthroquinones.[13] The upshot of these earlier studies is that a peri-substituted hydroxyl (i.e., 5-hydroxy or 5,8-dihydroxy in the naphthoquinones series) renders the quinone more easily reduced as a consequence of the LUMO-lowering effect of a geometrically favorable[14] internal H-bond. The ortho-hydroxylated (aminated) benzoquinones, on the other hand, do not consistently follow this trend. Unfortunately, the H-bond strength of the peri-hydroxyls cannot be modulated, and so these types of substrates cannot be employed to test the hypothesis that reduction potential scales with H-bond strength. However, the use of a series of naphthoquinones bearing peri-positioned *amide* units with deliberately varying H-bond donor capabilities can overcome this limitation and represents one approach by which the effect of varying H-bond strength on quinone reduction potential can be probed.

This premise was explored by synthesis of both unsymmetrically and symmetrically peri-functionalized 2,3-dimethylnaphthoquinones **5**–**9** and **11**–**13**, respectively, and correlation of salient molecular attributes reflecting H-bond strength with their half-wave reduction potentials. The syntheses of the target quinones were accomplished by modification of Diels Alder/oxidation chemistry reported by Fillion[15] using the mono amidobutadiene **4**[16] and the bis amidobutadiene **10**,[17] Scheme 1 (see Supplementary Data for details). In this chemistry, the efficiency of naphthoquinone formation was increased over prior work by consolidating the oxidation-cycloaddition-oxidation sequence into a single pot operation. Simply exposing the dihydroquinone **3** and the requisite diene to excess oxidant (MnO_2) furnished good yields of the desired naphthoquinone products **5** and **11**. These BOC-protected intermediates then served as branch points for the preparation of all of the other aminonaphthoquinone derivatives. All quinone products were characterized fully,[18] including single crystal X-ray for **8a** (Supplementary Data).[19] The X-ray derived structure clearly indicated the dominating effect of the N–H--O=C H-bond, which held the amide side chain in a coplanar orientation with the quinone framework.

Measurement of half-wave reduction potentials of the substituted naphthoquinones in CH_2Cl_2 led to the data shown in Table 1. These values were obtained under the following standard conditions: Pt disc electrode (1.6 mm diameter), $Ag/AgNO_3$ reference (0.01 M in CH_3CN), 2 mM in quinone, 100 mM in TBAP, 3 V/s, 0 to −2496 mV range, T = 20 °C. Under these conditions, ferrocenium ion exhibited a reduction potential of +200 mV (lit. 206 mV vs. $Ag/AgPF_6$)[20]. The IR frequency of the H-bond, which is well known to scale with H-bond strength, and the ^1H NMR H-bond signal position, a value also related to H-bond strength,[21] are reported in Table 1 as well. Concentration studies with **8a** over the span 1–100 mM revealed that neither the IR nor the ^1H NMR signal values varied significantly (± 1 cm^{-1}, and ± 0.05 ppm, respectively) throughout the experimental range.

Examination of these data reveals a clear correlation between the half-wave reduction potential and both H-bond strength metrics. However, a dissection of the two related effects that result when an amide is introduced onto the naphthoquinone framework is necessary in order to make further sense out of the data.

Both the (1) strong and directional H-bond between N–H and O=C and the (2) contributions of the nitrogen's lone pair via resonance with the carbonyl can play a role. Much precedent from the peri-*hydroxylated* cases suggest that H-bond activation of the carbonyl exerts the dominant influence, between these two interactions, on quinone reduction potential.[12a,13a-c,e] In an effort to probe the relative contributions of these two features in the amide substituted series examined herein, the controls **6**, **7**, **9a**, and **9b** were evaluated. In the absence of any electron-engaging carbonyl (amide) fu nctions, the nitrogen's lone pair certainly has the expected effect on the quinone's reduction potential, making it harder to reduce by 98 mV; compare entry *a* (R = H) with entry *b* (**6**, R = NH_2). In this instance, the N-H--O=C bond (IR absorption at 3339 cm^{-1}) can only be described as modest at best, and so this comparison is closest to a case where the H-bonding is turned off whereas the nitrogen lone pair contribution is turned on. Designing the complementary control (H-bonding turned off, nitrogen lone pair turned on) cannot be assured in this system due to uncertainty in the degree of overlap between the nitrogen's lone pair and the quinone, but entries **9a** and **9b**, where H-bonding has been abolished by methyl incorporation, come closest to approximating this goal. In these instances, the quinone reduction potential is depressed compared to the H-bonding analogues **8a**/**8b** by 76 mV (**8a** vs. **9a**) and 207 mV (**8b** vs. **9b**), respectively. In fact, the large difference between these values appears to be attributable primarily to the increased strength of the H-bond in the NHTFA case **8b**, as the reduction potentials of the H-bond incapable species **9a** and **9b** are essentially equivalent. From these data, it is apparent that whereas the nitrogen lone pair definitely contributes to depression of the quinone's reduction potential, its effects are relatively smaller that the H-bond effect and consistent throughout the relevant substrates. Therefore, the differences in measured reduction potential between the different acylated aminoquinone substrates should to a large measure reflect the impact of the H-bond, much as they do in the more well-studied peri-hydroxylated series.

Overall, the data for substrates **5, 8a, 8b, 11, 13a**, and **13b** do support the contention that quinone reduction potential correlates with the strength of the H-bond, but the imperfect measures of H-bond strength used for this correlation do little to encourage linearity. Double activation of the quinone function leads to increases in the reduction potential, as expected, but the amount of increase does not scale with increased H-bond strength. Thus, introducing an additional H-bond in the BOC species leads to an increase in reduction potential of 132 mV (entries *d* vs. *j*), whereas in the NHAc series (stronger H-bond), the difference is 125 mV (entries *e* vs. *k*) and in the NHTFA analogues (strongest H-bond), 239 mV (entries *f* vs. *l*). Extrapolation from these model compounds to photosynthetically relevant quinones embedded in protein matrices must be viewed with caution, but at the very least, the following hypotheses are supported by the data: (1) stronger N–H--O=C hydrogen bonds, as might be provided by H-bond networks in the enveloping proteins, makes the quinones more easily reduced, and (2) simultaneous N–H--O=C hydrogen bonding to both quinone carbonyls makes the quinones even more easily reduced than simple additivity might suggest.

Supplementary Material

Refer to Web version on PubMed Central for supplementary material.

Acknowledgment.

Funding via the National Institutes of Health, General Medical Sciences Division (GM 37861) and via the National Science Foundation for the X-Ray structural analysis facility (CHE-013111) is gratefully acknowledged.

References

1. Jordan P, Fromme P, Witt HT, Klukas O, Saenger W, Krauβ N. Nature 2001;411:909. [PubMed: 11418848]
2. Lancaster CRD, Bibikova MV, Sabatino P, Oesterhelt D, Michel H. J. Biol. Chem 2000;275:39364. [PubMed: 11005826]
3. Golbeck, JH., editor. Photosystem 1: The Light-Driven Plastocyanin:Ferredoxin Oxidoreductase. Springer; The Netherlands: 2006.
4. Ishikita H, Knapp E-W. J. Biol. Chem 2003;278:52002. [PubMed: 12972408]
5. Swallow, AJ. Function on Quinones in Energy Conserving Systems. Trumpower, BL., editor. Academic Press; New York, N.Y.: 1982. p. 59-72.
6. Kaupp M. Biochemistry 2002;41:2895. [PubMed: 11863427]
7. Pushkar YN, Golbeck JH, Stehlik D, Zimmermann H. J. Phys. Chem. B 2004;108:9439.
8. (a) Woodbury NW, Parson WW, Gunner MR, Prince RC, Dutton PL. Biochem. Biophys. Acta 1986:6. [PubMed: 3524681] (b) Prince RC, Dutton PL, Bruce JM. FEBS Lett 1983;160:273.
9. Sakuragi Y, Zybailov B, Shen G, Jones AD, Chitnis PR, van der Est A, Bittl R, Zech S, Stehlik D, Golbeck JH, Bryant DA. Biochemistry 2002;41:394. [PubMed: 11772039]
10. Howell JO, Goncalves JM, Amatore C, Klasnic L, Wightman RM, Kochi J. K. J. Am. Chem. Soc 1984;106:3968.The reduction potentials for **1** and models for **2** (i.e., menaquinone and **14a** in DMF were reported vs. a standard calomel electrode (SCE). These values were converted to NHE values by the formula $E_{(NHE)} = E_{(SCE)} + 240$ mV; see
11. (a) Gupta N, Linschitz H. J. Am. Chem. Soc 1997;119:6384. (b) Macías-Ruvalcaba N, Okamura N, Evans DH. J. Phys. Chem. B 2006;110:22043. [PubMed: 17064175]and references cited therein
12. (a) Edwards TG, Grinter R. Trans. Farad. Soc 1968;69:1070. (b) Aguilar-Martínez M, Cuevas G, Jiménez-Estrada M, González I, Lotina-Hennsen B, Macías-Ruvalcaba N. J. Org. Chem 1999;64:3684. [PubMed: 11674498] (c) Aguilar-Martínez M, Bautista-Martínez JA, Macías-Ruvalcaba N, González I, Tovar E, del Alizal Marín, Collera O, Cuevas G. J. Org. Chem 2001;66:8349. [PubMed: 11735513] (d) Macías-Ruvalcaba N, González I, Aguilar-Martínez M. J. Electrochem. Soc 2004;151:E110.
13. (a) Bezuglyi VD, Shapovalov VA, Fain VY. J. Gen. Chem., USSR (Eng. Trans) 1976;46:693. (b) Rao GM, Lown JW, Plambeck JA. J. Electrochem. Soc 1978;125:540. (c) Ashnagar A, Bruce JM, Dutton PL, Prince RC. Biochem. Biophys. Acta 1984;801:351. [PubMed: 6487650] (d) Crawford PW, Carlos E, Ellegood JC, Cheng CC, Dong Q, Liu DF, Luo YL. Electrochim. Acta 1996;41:2399. (e) Gómez M, González FJ, González I. J. Electroanal. Chem 2005;578:193.
14. (a) Schutte CJH, Paul SO, Smit RJ. Molec. Struct 1993;297:235. (b) Uno B, Okumura N, Goto M, Kano K. J. Org. Chem 2000;65:1448. [PubMed: 10814108] (c) Fukuzumi S, Kitaguchi H, Suenobu T, Ogo S. J. Chem. Soc., Chem. Commun 2002:1984.
15. (a) Chigr M, Fillion H, Rougny A, Berlion M, Riondel J, Beriel H. Chem. Pharm. Bull 1990;38:688. [PubMed: 2347011] (b) Potts KT, Bhattacharjee D. Synthesis 1983:31. (c) Schmidt RR, Wagner A. Synthesis 1981:273.See also
16. Overman LE, Taylor GF, Petty CB, Jessup PJ. J. Org. Chem 1978;43:2164.
17. Prepared in one pot (49%) by treatment of (*E*,*E*)-1,6-hexa-2,4-dienic diacid with $(PhO)_2PON_3$/Et_3N and t-BuOH at reflux; recrystallized from 80/20 EtOH/ H_2O. See the Supporting Data, and ref. 15c for the synthesis of a related compound
18. Banks JA, Cameron DW, Crossley MJ, Samuel EL. Aust. J. Chem 1976;29:2247.Compound **6**, with limited spectral data, has been reported
19. CCDC 649146 contains the supplementary crystallographic data for **8a**. These data can be obtained free of charge from The Cambridge Crystallographic Data Centre via www.ccdc.cam.ac.uk/data_request/cif.
20. Attia AS, Bhattacharya S, Pierpoint CG. Inorg. Chem 1995;34:4427.
21. Pimentel, GC.; McClellan, AL.; Freeman, WH. The Hydrogen Bond. San Francisco: 1960. (b) Takasuka M, Matsui Y. J. Chem. Soc., Perkin Trans. II 1979:1743. (c) Del Bene JE, Perera AA, Bartlett RJ. J. Phys. Chem. A 1999;103:8121.

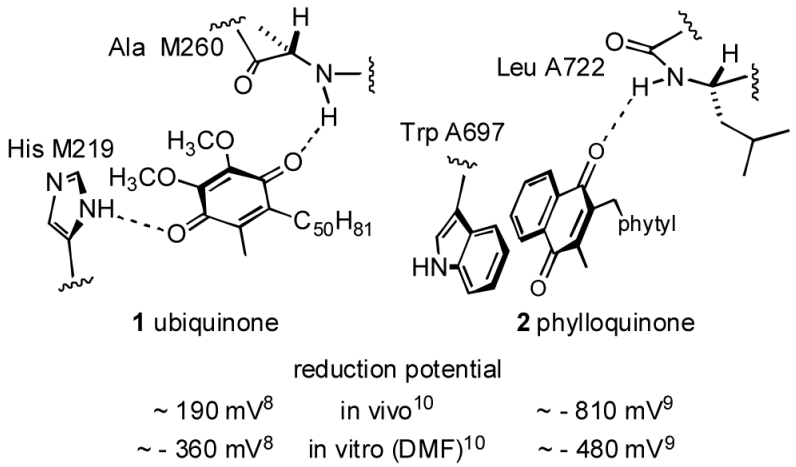

Figure 1.
Structures and figures of merit for the quinones of bRC (left) and PS1 (right). All reduction potentials are reported vs. the normal hydrogen electrode.[10]

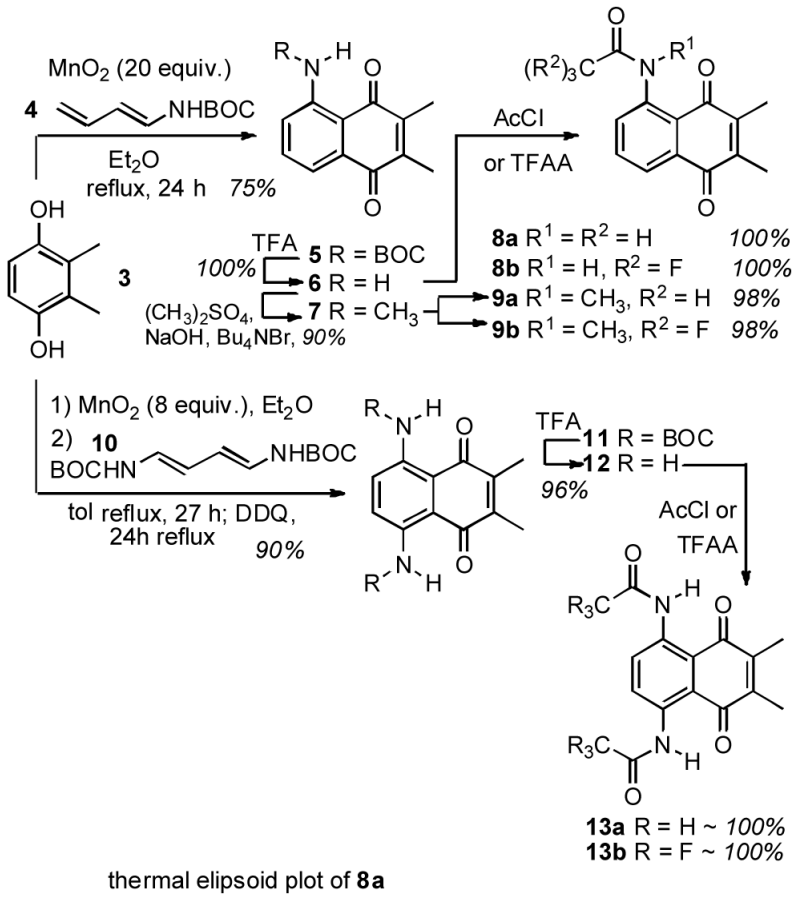

Scheme 1.

Synthesis of the target naphthoquinones **5**− **9**, and **11**−**13**; X-ray structure of **8a**. The thermal ellipsoid diagram (50% probability) was obtained with Bruker XSHELL software.

Table 1

Half-wave reduction potentials, salient IR frequencies, and ^{1}H NMR signal positions for the naphthoquinones 14.

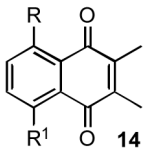

14

entry	cmpd. #	R	R^1	Red. Pot. (mV) CH_2Cl_2 [a]	N-H IR CCl_4 (cm^{-1})	N-H ^{1}H NMR C_6D_6 (δ)
a		H	H	-623	---	---
b	**6**	NH_2	H	-721	3339	not observed
c	**7**	$NHCH_3$	H	-697	3304	9.29
d	**5**	NHBOC	H	-551	3263	11.77
e	**8a**	NHAc	H	-484	3262	11.92
f	**8b**	NHTFA	H	-347	3109	13.08
g	**9a**	$N(CH_3)$ Ac	H	-560	---	---
h	**9b**	$N(CH_3)$TF A	H	-554	---	---
i	**12**	NH_2	NH_2	-819	3288	not observed
j	**11**	NHBOC	NHBOC	-419	3240	12.06
k	**13a**	NHAc	NHAc	-359	3201	12.18
l	**13b**	NHTFA	NHTFA	-108	3076	13.18

[a] All reduction potentials have been converted to NHE values via the formula: $E_{(NHE)} = E_{(AgNO3)}$ + 541 mV; see *Handbook of Analytical Chemistry*; Meites, L., Ed.; McGraw-Hill: New York, 1963.